Uniform peak optical conductivity in single-walled carbon nanotubes

Jesse M. Kinder* and Garnet Kin-Lic Chan
Department of Chemistry and Chemical Biology, Cornell University, Ithaca, New York 14853, USA

Jiwoong Park
Department of Chemistry and Chemical Biology, Cornell University, Ithaca, New York 14853 and
Kavli Institute at Cornell for Nanoscale Science, Ithaca, New York 14853, USA

(Received 2 February 2011; revised manuscript received 12 May 2011; published 12 September 2011)

Recent Rayleigh scattering measurements show that all single-walled carbon nanotubes have a peak optical conductivity of approximately 8 e^2/h, independent of radius, chiral angle, or whether the nanotube is semiconducting or metallic [D. Y. Joh *et al.*, Nat. Nanotechnol. **6**, 51 (2011)]. We show that this uniform peak conductivity is a consequence of the relativistic band structure and strength of the Coulomb interaction in carbon nanotubes. We also show that a simple exciton model accurately describes the general phenomenology and the numerical value of the peak optical conductivity. Our work illustrates the need for careful treatment of relaxation mechanisms in modeling the optoelectronic properties of carbon nanotubes.

DOI: 10.1103/PhysRevB.84.125428 PACS number(s): 78.67.Ch, 61.48.De, 71.35.−y, 78.35.+c

I. INTRODUCTION

Rayleigh scattering is a useful tool for studying the optical resonances of carbon nanotubes.[1,2] Using a new on-chip Rayleigh scattering technique, Joh *et al.* recently measured the peak optical conductivity for a variety of transitions in semiconducting and metallic nanotubes.[3,4] The sample included the second, third, and fourth exciton transitions in semiconducting nanotubes (S_{22}, S_{33}, and S_{44}) and the first and second exciton transitions in metallic nanotubes (M_{11} and M_{22}). The data obtained reveal a surprising phenomenon: the peak optical conductivity is independent of the nanotube radius and narrowly distributed around $\sigma_* = 8\ e^2/h$. The data are shown in Fig. 1.

The uniform response on resonance illustrated in Fig. 1 is significant because many physical properties of a nanotube depend strongly on its chiral index, the pair of integers that defines the arrangement of atoms in a nanotube. For instance, the wavelengths at which optical resonances occur are so strongly correlated with nanotube geometry that they can be used to identify the chiral indices of individual nanotubes in a sample.[5] In contrast, Joh *et al.* observed that, on resonance, *all* nanotubes responded like classical wires with the *same* conductivity.

In this paper, we explore the origin of this uniform peak conductivity. First, we show that linear response theory for the effective Dirac model of a carbon nanotube predicts a peak conductivity that is independent of the nanotube radius R whenever quasiparticle energies are proportional to $1/R$ and quasiparticle lifetimes are proportional to R. Next, we examine the lifetimes associated with several common scattering mechanisms in carbon nanotubes. We find that a simple exciton model with interband Coulomb scattering accounts for all the qualitative features of the data and provides an accurate estimate of the peak conductivity, while phonon and impurity scattering introduce only minor corrections. Finally, we discuss the limitations of this simple model for the lowest exciton transitions and for nanotubes with small diameters. Our analysis suggests that a uniform peak conductivity should be observable over a wide range of experimental conditions. Furthermore, it illustrates the importance of an accurate model of relaxation mechanisms in numerical studies of nanotube properties.

II. PEAK OPTICAL CONDUCTIVITY

Our starting point is the low-energy approximation to the tight-binding Hamiltonian for a carbon nanotube, which is a massless Dirac equation[6]

$$\mathcal{H} = \hbar v_F\, \mathbf{q}\cdot\boldsymbol{\sigma}, \tag{1}$$

where v_F is the Fermi velocity and $\mathbf{q}$ describes small displacements from the corners of the Brillouin zone of graphene. R is the only relevant length scale and defines a natural energy scale

$$E_0 = \hbar v_F/R. \tag{2}$$

The eigenvalues of $\mathcal{H}$ are $\pm E_0\sqrt{(kR)^2+\Delta^2}$, where k is the wave vector along the nanotube axis and Δ is the gap parameter. In metallic nanotubes, $\Delta = N$, and in semiconducting nanotubes, $\Delta = N \pm 1/3$. The band index N is an integer.

Scattering in nanotubes is dominated by light polarized along the nanotube axis,[7] which implies that the relevant quasiparticles are direct excitations of the form

$$|n\rangle = \sum_k A_{n,k} c_k^\dagger\, v_k |\Omega\rangle, \tag{3}$$

where $c^\dagger$ creates a conduction electron, $v^\dagger$ creates a valence electron, and $|\Omega\rangle$ is the ground state of filled valence orbitals. The excitation of a valence electron to the conduction band at wave vector k_0 is described by setting $A_{n,k}$ to $\delta_{k_0,k}$. The free-particle model can be extended to include the Coulomb interaction,[8] in which case the states defined by Eq. (3) form the basis of a single-band exciton model. The coefficients $A_{n,k}$ and exciton energies E_n are obtained as eigenvectors and eigenvalues of a Bethe-Salpeter equation. A single-band model such as this is sufficient to describe direct excitons (S_{ii} and M_{ii}) in carbon nanotubes.[9] Moreover, the scaling of the exciton size and binding energy within this model agrees with the results of *ab initio* calculations to leading order in

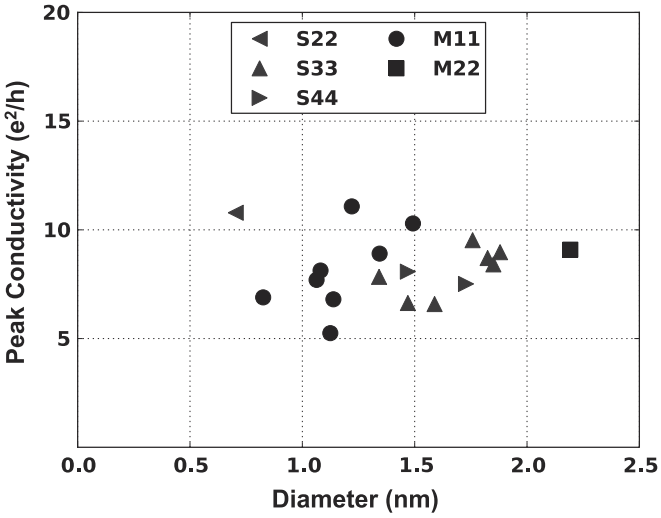

FIG. 1. Optical conductivity on resonance as a function of nanotube diameter, as measured by Joh *et al.* (Ref. 4). The mean value is $8 \pm 1.5\, e^2/h$, independent of the diameter.

R.[10,11] Therefore, a model based on Eq. (3) should accurately describe the dependence of the optical conductivity on the nanotube radius to leading order in R. [There are corrections of order $1/R^2$ to the exciton energies predicted by the Dirac model; there are also $1/R^2$ corrections to the exciton lifetime, as discussed in Sec. IV. Thus, corrections to predictions based on this model are expected to vanish as d/R tends to zero, where d is the carbon-carbon bond distance.]

At the level of linear response theory, the conductivity is given by the Kubo formula

$$\sigma(\omega) = \frac{\hbar e^2}{i\pi RL} \sum_n \frac{|\langle n|\hat{v}|\Omega\rangle|^2}{E_n} \frac{\hbar\omega + i\hbar\Gamma_n}{E_n^2 - (\hbar\omega + i\hbar\Gamma_n)^2}. \quad (4)$$

$\hat{v}$ is the velocity operator projected along the nanotube axis, and $\Gamma_n = 1/\tau_n$, where τ_n is the lifetime of the excited state. If $|n\rangle$ were eigenstates of the Hamiltonian in the absence of an applied field, Γ_n could be replaced by an infinitesimal to enforce causality. In practice, the exact eigenstates are never known. A broadening parameter $1/\tau$ is often introduced to account for relaxation. However, τ is not arbitrary: the broadening determines the optical conductivity on resonance, and different scattering mechanisms lead to qualitatively different quasiparticle lifetimes.

Although the conductivity is a tensor, only the surface current along the axis due to an electric field applied along the axis is considered here: $\sigma(\omega) \equiv \sigma_{zz}(\omega)$. Equation (4) gives the conductivity of a single band. The total conductivity is multiplied a factor of 2 for spin and a factor of 2 for the K and K' points.

The Kubo formula may be simplified by scaling all energies by E_0 and rewriting the expression in terms of the dimensionless parameters

$$w = \hbar\omega/E_0, \quad x_n = E_n/E_0, \quad y_n = \hbar\Gamma_n/E_0. \quad (5)$$

Equation (4) may be simplified further by introducing a dimensionless oscillator strength[8]

$$f_n = 2m^* \frac{|\langle n|\hat{v}|\Omega\rangle|^2}{E_n}. \quad (6)$$

The effective mass m^* is defined by $E_0 = m^* {v_F}^2$. The oscillator strengths for the solutions of the Dirac Hamiltonian satisfy a sum rule

$$\sum_k f_k = \frac{L}{\pi R}, \quad (7)$$

which follows from Eq. (6) when the sum over k is approximated by an integral. This sum rule also applies to excitons based on the free electron solutions of the Dirac equation. Thus, $f_n = \phi_n L/\pi R$, where ϕ_n is the fractional oscillator strength of the exciton transition.

Expressed as a function of the dimensionless parameters of Eq. (5) and the fractional oscillator strength, the Kubo formula becomes

$$\sigma(\omega) = \frac{e^2}{h} \frac{1}{i\pi} \sum_n \phi_n \frac{w + iy_n}{x_n^2 - (w + iy_n)^2}. \quad (8)$$

This expression implies $\sigma(\omega) = G(w;\boldsymbol{\lambda}) \cdot e^2/h$, where G is a dimensionless function and $\boldsymbol{\lambda}$ is a set of dimensionless parameters derived from $\{x_n\}$, $\{y_n\}$, and $\{\phi_n\}$. On resonance, w is a function of the other parameters so that $\sigma_* = G_*(\boldsymbol{\lambda}) \cdot e^2/h$. As we explain below, ϕ_n is independent of the nanotube radius. Therefore, if x_n and y_n are independent of the nanotube radius, then so is the peak conductivity. Equation (5) implies that x_n and y_n are independent of the nanotube radius if E_n and Γ_n are proportional to $1/R$, proving our central result: *If quasiparticle energies are inversely proportional to the nanotube radius and quasiparticle lifetimes are proportional to the nanotube radius, then the conductivity on resonance is independent of the nanotube radius.*

These arguments can be extended to multiple bands, indirect excitations, and unbound electron-hole pairs. [Although the fractional oscillator strength is no longer proportional to L/R for unbound electron-hole pairs, transforming the sum in Eq. (4) into an integral over k leads to the same result.]

Quasiparticle energies will be proportional to $1/R$ as long as Eq. (1) is a good approximation to the true single-electron Hamiltonian. The approximate many-body Hamiltonian is

$$\mathcal{H} = \sum_i \hbar v_F\, \boldsymbol{\sigma} \cdot \frac{\partial}{\partial \mathbf{r}_i} + \sum_{i<j} \frac{e^2}{\kappa |\mathbf{r}_i - \mathbf{r}_j|}, \quad (9)$$

where κ describes static screening from the environment and other bands of the nanotube. This Hamiltonian can also be expressed as

$$\mathcal{H} = \frac{\hbar v_F}{R} \left(\sum_i \boldsymbol{\sigma} \cdot \frac{\partial}{\partial \boldsymbol{\xi}_i} + \alpha \sum_{i<j} \frac{1}{|\boldsymbol{\xi}_i - \boldsymbol{\xi}_j|} \right), \quad (10)$$

where $\boldsymbol{\xi}_i = \mathbf{r}_i/R$ and $\alpha = e^2/2\pi\kappa\hbar v_F$ is an effective fine structure constant. Since the operator in parentheses is independent of R, its spectrum and eigenvectors are independent of R. Thus, quasiparticle energies are proportional to $1/R$, and quasiparticle wave functions are universal functions of

α, independent of R. (This also implies that the fractional oscillator strength is independent of R.) Because the inverse relation between the energy and the radius is a consequence of the relativistic band structure of Eq. (1), the first requirement for a uniform peak conductivity is not satisfied by all quantum wires and the effect may be specific to carbon nanotubes.

The second requirement for a peak conductivity that is independent of the nanotube radius is that quasiparticle lifetimes be proportional to the radius. Quasiparticle lifetimes arise from interactions not included in the Dirac equation, so the scaling arguments that ensure the energy scales as $1/R$ do not apply to the lifetime. Each interaction must be analyzed to determine how its contribution to the lifetime scales with the radius. In the next section, we show that quasiparticle lifetimes are not proportional to R in general, but intrinsic scattering mechanisms such as the Coulomb interaction and scattering from low-energy phonons do satisfy the second requirement.

III. QUASIPARTICLE LIFETIMES

The lifetime of a state $|n\rangle$ due to a potential V can be estimated from Fermi's golden rule:

$$\Gamma_n = (2\pi/\hbar)\sum_{m\neq n}|V_{m,n}|^2\delta(E_m - E_n). \tag{11}$$

The scattering rate can be factored into a product of two quantities

$$\Gamma(E) = \Gamma_0\gamma(E). \tag{12}$$

All of the dimensional quantities are factored out of the sum and collected into the base scattering rate Γ_0, and $\gamma(E)$ is a dimensionless function defined by the scaled sum. Regardless of the analytic form of $\gamma(E)$, the quasiparticle lifetime will be proportional to the radius if Γ_0 is proportional to $1/R$ and $\gamma(E)$ is independent of R.

Below, we analyze Coulomb scattering, phonon scattering, and impurity scattering. The Coulomb interaction largely determines the photophysics of carbon nanotubes. The absorption of a photon produces a particle-hole pair, and these charged particles interact strongly through their mutual Coulomb attraction. The interaction between particles and holes in the same band leads to strong exciton binding, and interband scattering gives the exciton a finite lifetime.[12] Other interactions also contribute to the exciton lifetime and may account for some of the spread in the data of Fig. 1. Intrinsic sources of scattering include phonons and lattice defects. External perturbations such as the substrate, applied fields, or atoms adsorbed on the surface of the nanotube also affect the conductivity.

A. Coulomb scattering

Kane and Mele considered interband Coulomb scattering in carbon nanotubes in Ref. 12. Adapting their analysis to Eq. (12), the base scattering rate is

$$\hbar\Gamma_0 = \alpha^2 E_0, \tag{13}$$

and $\gamma(E)$ is independent of R. Therefore, excitons that decay via interband Coulomb scattering will give rise to a peak conductivity that is independent of the radius. In fact, interband Coulomb scattering is sufficient to account for all of the qualitative features of the data: In a single-band exciton model with dissociation due to interband Coulomb scattering, the peak conductivity is independent of the radius, does not depend strongly on the transition responsible for the resonance, and is approximately equal in semiconducting and metallic nanotubes. Moreover, the value of the peak conductivity derived from the expression above is consistent with that measured by Joh *et al.*

If all the oscillator strength of a band were localized in a single exciton transition and $\gamma(E) = 1$, then the peak conductivity would be

$$\sigma_* = \frac{e^2}{h}\frac{2\kappa^2}{\pi\alpha_0{}^2}, \tag{14}$$

where $\alpha_0 = e^2/2\pi\hbar v_F \approx 0.42$, and κ is the dielectric constant of the environment. The experimental measurements shown in Fig. 1 were taken on a quartz substrate in glycerol ($n = 1.46$). Setting $\kappa = n^2$ gives a maximum conductivity of $\sigma_* \approx 16\,e^2/h$. Not all of the oscillator strength is localized in a single exciton transition, but *ab initio* calculations indicate that the lowest exciton transition accounts for 50% to 70% of the total oscillator strength.[10] The lower end of this range gives a peak conductivity of $8\,e^2/h$, consistent with the experiment.

For most of the transitions probed in the experiment, $\gamma(E)$ is close to 1, and the expression above gives an accurate estimate of the peak conductivity. However, Eq. (14) does *not* apply to the peak conductivities of the S_{11} and S_{22} transitions in semiconducting nanotubes. We discuss this in the next section.

Another feature of the data that emerges from the exciton model is the similar peak conductivities in semiconducting and metallic nanotubes. The bands in metallic nanotubes are twofold degenerate, which suggests the peak conductivity of metallic nanotubes could be twice that of semiconducting nanotubes. However, screening in metallic nanotubes reduces the exciton binding energy and oscillator strength, which leads to similar peak conductivities in metallic and semiconducting nanotubes.

A single-band exciton model with dissociation due to interband Coulomb scattering accounts for all the qualitative features of Fig. 1, and Eq. (14) can be used to estimate the peak conductivity in different dielectric environments. Phonon and impurity scattering will introduce minor corrections to these estimates.

B. Phonon scattering

Electron-phonon interactions are another significant source of scattering in carbon nanotubes.[13–17] The excitation of a phonon deforms the carbon lattice, which introduces an effective potential to the Dirac Hamiltonian of Eq. (1).[6,18] Variations in the lattice charge density can produce a scalar deformation potential, and bending and stretching of bonds can introduce an effective gauge potential. Because the orientation of the bonds with respect to the axis of a nanotube depends on its geometric structure, the gauge potential and the associated phonon scattering rates depend on the chiral angle θ_c. The estimates of the contribution of phonon scattering to the peak conductivity given below are based on the effective potentials of Ref. 18.

At room temperature, only the low-energy phonons are populated: the acoustic modes and the radial breathing mode. There are four acoustic modes in carbon nanotubes. The longitudinal acoustic (LA) modes compress and expand the lattice along the nanotube axis. The transverse acoustic (TA) or twist modes rotate the lattice about the nanotube axis. Both of these modes have a linear dispersion relation $\omega_q = cq$, where c is the sound velocity. These modes do not carry any angular momentum and lead to small-momentum scattering within a band. The two flexure modes bend the nanotube in the plane of its axis. These modes have a quadratic dispersion relation $\omega_q = cq^2R$, where c has units of velocity. These modes carry one quantum of angular momentum and mediate interband transitions. The radial breathing mode (RBM) is a periodic variation in the radius of a nanotube along its axis. Its frequency is inversely proportional to the nanotube radius. At small wave vector, $\omega_q \approx c/R$, where c has units of velocity. For the acoustic modes and the RBM, c is on the order of 10 km/s.[18–20]

The scattering rates of the RBM, LA, TA, and flexure modes all have the same general form. In the high-temperature limit, the base scattering rate is

$$\hbar\Gamma_0 = \frac{g^2 k_B T}{4\pi\hbar\rho_0 c^2 v_F R}. \tag{15}$$

In the zero-temperature limit,

$$\hbar\Gamma_0 = \frac{g^2}{4\pi\rho_0 c v_F R^2}. \tag{16}$$

Here, g characterizes the strength of the electron-phonon interaction, T is the temperature, and ρ_0 is the mass density of the graphene lattice. $\gamma(E)$ of Eq. (12) depends on the ratio of the phonon and Fermi velocities c/v_F and the chiral angle θ_c, but not R. As a result, the contribution of these modes to the peak conductivity is independent of the radius in the high-temperature limit. Although a single parameter g appears above, the strength of the deformation potential is on the order of 20 eV, while the gauge potential is of order 2 eV.[18] As a result, the LA and RB modes, which contribute to the deformation potential, generally have larger scattering rates than the other modes.

The base rate of acoustic and RBM phonon scattering is roughly two orders of magnitude smaller than the rate of interband Coulomb scattering. For a dielectric with $\kappa \approx 2$, Eq. (13) gives a base Coulomb scattering rate of $\hbar\Gamma_c \approx 20$ meV. Taking $g \sim 20$ eV (for phonon modes that contribute to the deformation potential) gives $\hbar\Gamma_{ph} \approx 0.6$ meV, or about 3% of the Coulomb scattering rate. The scattering rate of modes that only contribute to the gauge potential, the TA and flexure modes, is smaller by two orders of magnitude. Although there is some uncertainty in the strength of the electron-phonon coupling, measurements of the dc conductivity in metallic nanotubes give a room-temperature acoustic phonon scattering rate of $\hbar\Gamma_{ph} \approx 1$ meV,[14] about 5% of the interband Coulomb scattering rate. Thus, the peak conductivity is probably determined primarily by interband Coulomb scattering, with small variations due to scattering from acoustic and RBM phonons.

Analyzing variations in the peak conductivity as a function of temperature might provide a way to extract the contributions of different phonon modes to the peak conductivity. The contribution of the RBM should show a crossover to radius-dependent scaling as the temperature is reduced, and the contribution of the other acoustic modes should scale linearly with temperature. At room temperature, these variations should be on the order of a few percent of the peak conductivity.

Optical phonons also introduce a gauge potential to the Dirac Hamiltonian, and their contribution to the scattering rate can be calculated within the same theoretical framework. (Optical phonons do not contribute to the scalar potential. The motion of the two sublattices is out of phase, so there is no long-wavelength variation in the lattice charge density.) The dispersion relation of an optical phonon is constant for small wave vectors: $\omega = \Omega_0$. Unlike the acoustic modes and the RBM, the dispersion relation is independent of the nanotube radius. The resulting scattering rates do not satisfy the criteria for a uniform peak conductivity. $\gamma(E)$ depends on $R\Omega_0/v_F$ for all optical phonon scattering processes, which leads to nonuniform scaling of quasiparticle lifetimes with the nanotube radius. In addition, the base scattering rate Γ_0 does not scale as $1/R$ for some optical modes.

Only the zero-temperature limit is relevant for optical phonons: for the LO and TO modes, $\hbar\Omega_0 \approx 200$ meV, and the optical analog of the RBM, the RO mode, has $\hbar\Omega_0 \approx 100$ meV.[20] The base scattering rate for the LO and TO modes is

$$\hbar\Gamma_0 = \frac{g^2}{4\pi\rho_0\Omega_0 v_F R d^2}, \tag{17}$$

where $d \approx 0.15$ nm is the carbon-carbon bond length. For a nanotube with a radius of 1 nm, $\hbar\Gamma_0 \approx 10$ μeV. For the RO mode,

$$\hbar\Gamma_0 = \frac{g^2}{4\pi\rho_0\Omega_0 v_F R^3}, \tag{18}$$

which is smaller than the base rate of the LO and TO modes by two orders of magnitude. Although optical modes violate the conditions required for a uniform peak conductivity, their contribution to the overall scattering rate is negligible.

C. Impurity scattering

Short-range potentials in the nanotube or its environment provide another source of scattering. A potential with a range smaller than the nanotube radius can be approximated as a two-dimensional impurity, i.e., a pointlike defect on the surface of the nanotube: $V(\mathbf{r}) \approx V_0 a^2 \delta(\mathbf{r})$, where $a \lesssim R$ is the range of the potential. This might represent a topological defect in the lattice, a substitution impurity at a lattice site, or an atom adsorbed on the surface of the nanotube. [If the potential affects the two sublattices differently, the scalar V_0 can be replaced by a 2×2 matrix $V_0\,\hat{\mathbf{n}}\cdot\boldsymbol{\sigma}$. This does not affect the base scattering rate Γ_0, but may introduce some dependence on the chiral angle in $\gamma(E)$.] Incoherent elastic scattering from identical impurities gives a base scattering rate proportional to $1/R$:

$$\hbar\Gamma_0 = \frac{\nu a^4 {V_0}^2}{2\pi\hbar v_F R}, \tag{19}$$

where ν is the surface defect density.

A longer-range potential that is nearly uniform around the circumference of a nanotube, but whose range is small compared with the wavelength of a particle ($ka \ll 1$), may be approximated by a one-dimensional impurity potential: $V(\mathbf{r}) \approx a V_0\, \delta(z)$. Here, V_0 is the average potential around the circumference. This potential might approximate a charge defect in the substrate or a local gating potential. The resulting scattering rate is *independent* of the radius

$$\hbar\Gamma_0 = \frac{\lambda a^2 {V_0}^2}{\hbar v_F}, \tag{20}$$

where λ is the linear defect density.

For elastic scattering processes, $\gamma(E)$ of Eq. (12) is independent of the nanotube radius. However, impurity scattering will be inelastic if it involves an Auger process or leads to the excitation of a vibrational mode, an atomic transition, or a change in the molecular configuration of the scattering center. For inelastic scattering processes that involve an internal excitation of the impurity with energy $\hbar\Omega_0$, $\gamma(E)$ depends on $R\Omega_0/v_F$, violating the conditions for a uniform peak conductivity. Thus, elastic scattering from short-range 2D impurities contributes to a peak conductivity that is independent of the radius; inelastic scattering and long-range impurity scattering contribute to a peak conductivity that depends on the radius.

To estimate the importance of impurity scattering, we consider a short-range impurity with $V_0 = 1$ eV and a range of 1 Å. An extremely high defect density of 1 per nm^2 then gives a scattering rate that is smaller than the Coulomb scattering rate by three orders of magnitude. For a long-range impurity with a range of 1 nm, a density of 1 per μm is necessary to generate a scattering rate comparable to that of interband Coulomb scattering. The high mobilities observed in dc transport measurements suggest that impurity scattering of any type is insignificant compared with phonon scattering.[13,14] Under typical experimental conditions, defect densities are probably too low to have a significant effect on the peak conductivity.

IV. DISCUSSION

We have demonstrated that the peak conductivity will be independent of the radius of a carbon nanotube if quasiparticle energies are proportional to $1/R$ and quasiparticle lifetimes are proportional to R. We have also showed that a simple exciton model with dissociation due to interband Coulomb scattering can account for most features of the experimental data. In this section, we address the limitations of this simple model. Significant deviations are possible in two cases. First, trigonal warping will introduce chiral angle-dependent variations in the peak conductivity. Second, the peak conductivity of the two lowest excitons in a semiconducting nanotube could be significantly greater than that of higher excitations.

Trigonal warping refers to corrections to Eq. (1) that break the full rotational symmetry of the graphene spectrum near the Dirac points down to the threefold rotational symmetry of the underlying honeycomb lattice. This introduces corrections to the dispersion relation of carbon nanotubes of order $E_0 d/R$, where d is the carbon-carbon bond length. The Dirac Hamiltonian is a good approximation to the true Hamiltonian for a nanotube with a radius much larger than the lattice spacing lattice spacing, but when the radius is smaller than about 1 nm, corrections due to trigonal warping are significant, especially in higher subbands.

Trigonal warping is responsible for $1/R^2$ corrections to the $1/R$ scaling of exciton energies.[9–11] Since most of the oscillator strength is concentrated in a single exciton transition, shifts in the exciton *energies* have little effect on the peak conductivity. However, trigonal warping also introduces variations in exciton *lifetimes*, and this will lead to variations in the peak conductivity that depend on the chiral angle and decrease as the nanotube radius increases. This could explain some of the spread in Fig. 1, but the small sample size and limited range of diameters are insufficient to establish any definite relationship between variations in the peak conductivity and the radius or chiral angle of the nanotubes. (The structural information for the nanotubes in the sample can be found in the supplemental information of Ref. 4.)

In addition to trigonal warping, differences in the decay channels available to low-lying excitons could lead to significant deviations from a uniform peak conductivity. The data set in Fig. 1 consists primarily of S_{33}, S_{44}, and M_{11} transitions. Although the peak conductivities of these transitions show a surprising degree of uniformity, this does not imply that *all* exciton transitions will have a peak conductivity of $8\, e^2/h$.

The S_{22} transition could have a larger peak conductivity than higher-lying excitons, even though the dominant relaxation mechanism is interband Coulomb scattering. The lifetime of an exciton can be approximated by the lifetime of a particle-hole pair at the band edge, as in Ref. 12. For a transition between bands m and n,

$$\gamma_{nm} \propto \left(1 + \frac{\Delta_m}{\Delta_n}\right)^2 I^2_{|m-n|}(\xi)\, K^2_{|m-n|}(\xi), \tag{21}$$

where $\xi^2 = \Delta_n^2 - \Delta_m^2$, and $I_n(x)$ and $K_n(x)$ are modified Bessel functions. The total scattering rate for an exciton is given by the sum of the rates for transitions to all bands with $|\Delta_m| < |\Delta_n|$. Except for the two lowest-lying excitons in semiconducting nanotubes, this sum is close to 1: for the S_{33}, S_{44}, M_{11}, and M_{22} excitons, its value is between 0.7 and 1.2. This is consistent with the uniform peak conductivities in Fig. 1.

For the S_{22} exciton, only scattering into the lowest band is allowed by conservation of energy. Although the base scattering rate Γ_0 is the same for S_{22} and higher-lying excitons, the scattering rate is smaller because the gap parameters of the first and second bands have opposite signs. This leads to a small value of $\gamma(E)$ in Eq. (21). In contrast, all higher-lying excitons have at least one decay channel into a band with a gap parameter of the same sign. Because the dominant contribution to the exciton lifetime is interband Coulomb scattering, the peak conductivity of S_{22} transitions *is* expected to be uniform across a sample of nanotubes with different diameters and chiralities. However, Eq. (21) predicts that it will be three to four times larger than that of higher-lying excitations. The single S_{22} transition in Fig. 1 has a peak conductivity of $10.8\, e^2/h$. This is larger than the mean, but smaller than predicted by the Dirac model. Corrections due to trigonal warping may account for this discrepancy: the nanotube has a radius of just 0.35 nm.

Due to conservation of energy, the S_{11} exciton can not decay via interband Coulomb scattering. Thus, the estimate of the peak conductivity in Eq. (14) does not apply. The important relaxation pathways for this exciton are not fully understood. At high exciton densities, two-exciton Auger recombination is the dominant mechanism.[21] At low exciton densities, possibilities include nonradiative recombination mediated by phonons or free electrons and holes.[22,23] Depending on the decay channel, the peak conductivity of the S_{11} exciton may not be uniform across a nanotube sample, and may differ significantly from $8\ e^2/h$. No experimental data are available for this transition. For nanotubes with diameters on the order of 1 nm, the S_{11} transition lies in the infrared, and this region of the spectrum has not been probed in Rayleigh scattering measurements.

V. CONCLUSION

To summarize, we have shown that linear response theory applied to the effective Dirac Hamiltonian for carbon nanotubes predicts a peak conductivity that is independent of the nanotube radius whenever quasiparticle energies are inversely proportional to the nanotube radius and quasiparticle lifetimes are proportional to the radius. The relativistic band structure of carbon nanotubes leads to quasiparticle energies that are proportional to the fundamental energy scale $\hbar v_F/R$, and exciton dissociation due to interband Coulomb scattering is consistent with both the uniformity and mean value of the peak conductivities measured by Joh *et al.*[4] Phonon scattering, impurity scattering, and trigonal warping may account for variations between nanotubes probed in the experimental sample. Furthermore, the peak conductivity of S_{11} and S_{22} excitons could be significantly larger than $8\ e^2/h$ due to differences in the available decay channels.

Our analysis suggests that the peak conductivity at optical wavelengths will be *uniform* over a wide range of experimental conditions: it will be the same for all nanotubes in a sample, independent of diameter, chiral angle, or whether the nanotube is semiconducting or metallic. The peak conductivity is not *universal*, however, and may depend on factors such as the dielectric environment, temperature, or doping.

A uniform peak conductivity could be useful in optical devices that utilize carbon nanotubes. Many properties of a nanotube depend strongly on its radius and vary significantly between semiconducting and metallic nanotubes. Applications designed to exploit these properties are faced with the difficult task of separating nanotubes based on their geometry. In applications that only depend on the resonant conductivity, nanotubes would be interchangeable: on resonance, all nanotubes behave as classical wires (hollow conducting cylinders) with the *same* conductivity.

Our analysis of quasiparticle lifetimes illustrates the importance of the broadening term in numerical studies. A scattering rate inversely proportional to the nanotube radius is essential to reproduce the uniform conductivity observed by Joh *et al.* In calculations of nanotube properties, it is common to introduce a phenomenological broadening parameter to account for scattering mechanisms not included in the model. However, different mechanisms give rise to different scaling relations between quasiparticle lifetimes and the nanotube radius. Using the same broadening parameter for all nanotubes can yield incorrect predictions for the relation between the material properties of a carbon nanotube and its geometry. To fit an experimental data set, a separate phenomenological broadening parameter could be adjusted for each nanotube. The experiments of Joh *et al.* and the analysis above suggest a simpler approach. For a given set of experimental conditions, a single parameter τ_0 can describe all nanotubes in a sample if the lifetime is taken to be proportional to the nanotube radius: $\tau = \tau_0(R/R_0)$.

ACKNOWLEDGMENTS

J.M.K. would like to thank D. Joh and L. Hermann for many helpful discussions of the experiment. This work was funded by the Cornell Center for Materials Research, the Center for Molecular Interfacing, the NSF CAREER grant, the Air Force Office of Scientific Research (NE and IO), the Camille and Henry Dreyfus Foundation, the David and Lucile Packard Foundation, and the Alfred P. Sloan Foundation.

*jk959@cornell.edu

[1] M. Sfeir, F. Wang, L. Huang, C. Chuang, J. Hone, S. O'Brien, T. Heinz, and L. Brus, Science **306**, 1540 (2004).
[2] S. Berciaud, C. Voisin, H. Yan, B. Chandra, R. Caldwell, Y. Shan, L. E. Brus, J. Hone, and T. F. Heinz, Phys. Rev. B **81**, 041414 (2010).
[3] D. Y. Joh, L. H. Herman, S.-Y. Ju, J. Kinder, M. A. Segal, J. N. Johnson, G. K. L. Chan, and J. Park, Nano Lett. **11**, 1 (2011).
[4] D. Y. Joh, J. Kinder, L. H. Herman, S.-Y. Ju, M. A. Segal, J. N. Johnson, G. K. L. Chan, and J. Park, Nat. Nanotechnol. **6**, 51 (2011).
[5] S. M. Bachilo, M. S. Strano, C. Kittrell, R. H. Hauge, R. E. Smalley, and R. B. Weisman, Science **298**, 2361 (2002).
[6] C. L. Kane and E. J. Mele, Phys. Rev. Lett. **78**, 1932 (1997).
[7] M. F. Islam, D. E. Milkie, C. L. Kane, A. G. Yodh, and J. M. Kikkawa, Phys. Rev. Lett. **93**, 37404 (2004).
[8] T. Ando, J. Phys. Soc. Jpn. **66**, 1066 (1997).
[9] M. Dresselhaus, G. Dresselhaus, R. Saito, and A. Jorio, Annu. Rev. Phys. Chem. **58**, 719 (2007).
[10] V. Perebeinos, J. Tersoff, and P. Avouris, Phys. Rev. Lett. **92**, 257402 (2004).
[11] R. B. Capaz, C. D. Spataru, S. Ismail-Beigi, and S. G. Louie, Phys. Rev. B **74**, 121401 (2006).
[12] C. L. Kane and E. J. Mele, Phys. Rev. Lett. **90**, 207401 (2003).
[13] J. Park, S. Rosenblatt, Y. Yaish, V. Sazonova, H. Üstünel, S. Braig, T. Arias, P. Brouwer, and P. McEuen, Nano Lett. **4**, 517 (2004).
[14] X. Zhou, J. Park, S. Huang, J. Liu, and P. McEuen, Phys. Rev. Lett. **95**, 146805 (2005).
[15] M. Dresselhaus, G. Dresselhaus, R. Saito, and A. Jorio, Phys. Rep. **409**, 47 (2005).

[16]V. Perebeinos, J. Tersoff, and P. Avouris, Phys. Rev. Lett. **94**, 27402 (2005).
[17]Y. Miyauchi and S. Maruyama, Phys. Rev. B **74**, 35415 (2006).
[18]H. Suzuura and T. Ando, Phys. Rev. B **65**, 235412 (2002).
[19]J. Lischner and T. A. Arias, Phys. Rev. B **81**, 233409 (2010).
[20]R. Saito, G. Dresselhaus, and M. Dresselhaus, *Physical Properties of Carbon Nanotubes* (Imperial College Press, London, 1999).
[21]Y. Ma, J. Stenger, J. Zimmermann, S. Bachilo, R. Smalley, R. Weisman, and G. Fleming, J. Chem. Phys. **120**, 3368 (2004).
[22]V. Perebeinos and P. Avouris, Phys. Rev. Lett. **101**, 057401 (2008).
[23]J. M. Kinder and E. J. Mele, Phys. Rev. B **78**, 155429 (2008).